Improved Implementation of the Frequency Hopped Code Selection DFRC Scheme

Elias Aboutanios†, William Baxter†, Yimin D. Zhang‡

† School of Electrical and Telecommunications Engineering, University of New South Wales Australia
‡ Department of Electrical and Computer Engineering, Temple University, Philadelphia, PA 19122, USA

E-mails: elias@ieee.org, w.baxter@unsw.edu.au, ydzhang@temple.edu

***Abstract*—Dual-function radar-communications (DRFC) strategies aim to embed communication symbols into the radar waveforms, which serve to alleviate the spectrum congestion problem. In this context, frequency-hopping code selection (FHCS) has been proposed as an effective DFRC approach in frequency-hopped multiple-input multiple-output (MIMO) radar. FHCS encodes the communication symbols through the selection from the available hops of the subset of hops to be assigned to the waveforms in each chip. In this manner, FHCS applies information embedding in the fast-time, thereby greatly increasing the achievable bit rate at the expense of increased impact on the radar performance. In this work, we propose an enhanced version of the FHCS scheme that ameliorates the resulting ambiguity function, thus improving the radar performance. Furthermore, we present a practical implementation scheme that employs a greedy divide-and-conquer approach. The performance of the proposed strategy is evaluated using simulations and the benefits to the radar ambiguity function are demonstrated.**

I. Introduction

Dual-function radar-communications (DFRC) strategies aim to host a communication function alongside the radar operation, which is maintained as the primary function [1]. Thus, DFRC strategies prioritize the sensing modality of the host radar platform and proceed to parasitically embed information symbols into the radar waveforms [2], [3]. In this way, proper DFRC system design allows the communication function to capitalize on the radar infrastructure with little or no impact on the primary sensing operation.

A number of DFRC strategies have been proposed to date [4]–[11]. Seeking to preserve the main beam operation of the radar, sidelobe modulation was employed to embed communication symbols via the manipulation of the sidelobe level (SLL) [4], [12]. To exploit the higher signal power of the mainlobe, the phase modulation (PM) approach embeds communications symbols in the main beam while preserving the spectral profile of the radar waveform [13], [14].

Multiple-input multiple-output (MIMO) radar has attracted significant attention within the DFRC context as the increased number of degrees of freedom (DoFs) offered by the MIMO array configurations can be leveraged to develop improved information embedding schemes [2], [15]. Thus, phase-shift keying (PSK) [16], [17] and amplitude-shift keying (ASK) [18], [19] modulation schemes have been proposed to service the communication function. These increased DoFs have also opened up the way for index modulation schemes utilizing non-traditional symbol sets, such as the transmit radar signal or the transmit elements [5], [8], [20], [21]. For example, the strategy of waveform shuffling (or permutation) encodes the communications symbols via the assignment of the orthogonal MIMO waveforms to the transmit elements in the array [5], [8] without affecting the radar operation. Since the order of the waveforms is known by the radar, it can be reversed at the radar receiver, thus ensuring that the shuffling does not affect the radar operation. At the communication receiver, the transmitted symbol is determined by finding the correct order.

The schemes discussed so far embed information in slow-time meaning that each pulse conveys one communication symbol. This allows them to preserve the radar waveform but limits their achievable bit rates by the radar pulse repetition frequency (PRF). This limitation can be circumvented if symbol embedding is implemented in fast-time. This has motivated the use of frequency-hopped (FH) waveforms in MIMO radars for DFRC systems, where subpulse modulation yields significantly higher bit rates [7], [9], [22]–[24]. In [7], PSK symbols were embedded by modulating the phases of the FH subpulses while in [25] differential phase-shift keying (DPSK) was used. An alternative strategy employing index modulation via carrier selection was proposed in [9] where the frequency hops themselves were used to indicate the communication symbols. Referred to as the frequency-hopping code selection (FHCS) scheme, each symbol is embedded into the series of hops comprising the set of FH-MIMO radar waveforms. The FHCS scheme was then combined with an index modulation scheme to provide a simultaneous boost in data rates and communication secrecy [26]. More recently, a generalized framework for information embedding in an FH-MIMO DFRC system was presented in [27]. This generalized framework includes the aforementioned schemes as special cases and permits hybrid modulation schemes to be devised.

While these fast-time approaches endow the FH-MIMO DFRC system with superior data rates, encoding information symbols in the radar fast-time can have deleterious effects on the primary sensing operation [27], [28]. For instance, the PSK scheme presented in [7] introduces abrupt phase transitions between consecutive subpulses, leading to out-ofband leakage accompanied with an increase in the spectral sidelobe level [29], [30]. To better manage the phase discontinuities at the subpulse boundaries, [31] employed code-shift keying (CSK) with the optimum sequence of CSK-modulated symbols, which jointly optimize the radar and communications performance, are derived using a genetic algorithm. The optimized CSK sequences result in lower range sidelobes in the ambiguity function (AF) response than the PSK scheme reported in [7]. However, these sequences are optimized only once and are not updated every coherent processing interval. In the case of the FHCS scheme, the impact of the fast-time information embedding on the radar performance was explored in [32] through the possibility of waveform degeneration. This is due to the selection of the FH symbols by the communication function which may result in an increase in the number of repeated hops within the pulse. In this respect, the codebook design, including the dictionary truncation and the subsequent arrangement of the hops, becomes an important task. Consequently, dictionary balancing was proposed to reduce the probability of waveform degeneration and improve the AF [32].

In contrast to the strategy developed in [32], where the dictionary balancing is carried out and the dictionary is subsequently fixed, we propose in this paper to balance the symbols on a pulse-by-pulse basis to improve the radar AF profile. Thus, instead of achieving improvement on average, which is independent of the symbol selection for the particular pulse, the proposed approach to adaptively balance the specific symbols chosen by the communication function within the pulse would lead to further improvement in the AFs. We give a heuristic algorithm that spreads the hops evenly over the waveforms in order to reduce the first sidelobe (delay of one subpulse) and verify the performance via simulations.

The paper is organized as follows: In Section II we present the signal model in a FH-MIMO radar. Section III describes the FHCS scheme, and Section IV discusses the dictionary truncation, waveform degeneration, and dictionary balancing approaches. The proposed pulse balancing strategy is then described in Section V. Numerical results are presented in Section VI to demonstrate the performance. Finally, conclusions are drawn in Section VII.

II. MIMO Radar Signal Model

A MIMO radar equipped with colocated transmit and receive linear arrays of M and N isotropic antennas, respectively, emits a burst of pulses with pulse width T_{w} and pulse repetition interval T_p, giving a pulse duty cycle $D = (T_{\mathrm{w}}/T_{\mathrm{p}})\times 100\%$. For MIMO operations, the transmit waveforms $\phi_m(t)$, $m = 1, \ldots, M$, should satisfy the orthogonality condition [33]

$$\int_0^{T_{\mathrm{w}}} \phi_m(t)\phi^*_{m'}(t+\tau)e^{j2\pi\nu t}dt = \begin{cases} \delta(\tau)\delta(\nu), & m = m', \\ 0, & \text{otherwise}, \end{cases} \tag{1}$$

where τ and ν are the time delay and Doppler, and $(\cdot)^*$ denotes complex conjugate. Then, the $N \times 1$ receive signal vector due to the reflection by a target located at direction θ is

$$\mathbf{x}(t,n) = \alpha(n)\left[\mathbf{a}^T(\theta)\boldsymbol{\phi}(t)\right]\mathbf{b}(\theta) + \mathbf{z}(t,n), \tag{2}$$

where n is the pulse index, $\alpha(n)$ is the reflection coefficient of the target during the nth pulse, and $\mathbf{a}(\theta)$ and $\mathbf{b}(\theta)$ denote the steering vectors of the transmit and receive arrays, respectively, and $(\cdot)^T$ denotes matrix or vector transpose. In addition, $\boldsymbol{\phi}(t) \triangleq [\phi_1(t), \ldots, \phi_M(t)]^T$ is the complex vector of orthogonal waveforms and $\mathbf{z}(t,\tau)$ is an $N \times 1$ vector of zero-mean white Gaussian noise. In what follows we assume that the reflection coefficient $\alpha(n)$ conforms to the Swerling II target model [34], that is, it remains constant during the pulse duration but varies independently from pulse to pulse.

Following matched filtering with the transmit waveforms we obtain the length-MN extended signal vector

$$\mathbf{y}(n) = \alpha(n)[\mathbf{a}(\theta) \otimes \mathbf{b}(\theta)] + \tilde{\mathbf{z}}(n), \tag{3}$$

where $\otimes$ is the Kronecker product and $\tilde{\mathbf{z}}(n)$ is the output additive zero-mean Gaussian noise with covariance $\sigma_z^2\mathbf{I}_{MN}$ with $\mathbf{I}_{MN}$ being the $MN \times MN$ identity matrix.

As truly orthogonal waveforms are impossible to achieve in practice, FH waveforms have been extensively studied as quasi-orthogonal waveforms for MIMO operations. The pulse in an FH-MIMO radar is divided into Q chips or subpulses of duration $\Delta_t = T_{\mathrm{w}}/Q$. The bandwidth BW Hz that is available to the radar is divided into K subcarriers that are spaced by Δ_f such that $K\Delta_f \leq BW$. Then, the mth FH waveform can be expressed as

$$\phi_m(t) = \sum_{q=0}^{Q-1} e^{j2\pi c_{m,q}\Delta_f t}\Pi(t - q\Delta_t), \tag{4}$$

where $c_{m,q}$, $m = 1, \cdots, M$, $q = 0, \ldots, Q-1$, are the indices of frequency hops, drawn from the set of non-negative integers $\mathbb{K} \triangleq \{0, 1, \ldots, K-1\}$, and the rectangular function $\Pi_q(t)$ is defined as

$$\Pi_q(t) \equiv \Pi(t - q\Delta_t) \triangleq \begin{cases} 1, & q\Delta_t \leq t \leq (q+1)\Delta_t, \\ 0, & \text{otherwise}. \end{cases} \tag{5}$$

While the radar operation dictates that the FH waveforms are pre-designed and remain fixed, this requirement is relaxed in order to permit information embedding in fast-time. This will be described in the next section.

III. Information Embedding in FH-MIMO Radar

Granted the freedom to manipulate all of the amplitudes, phases, and frequencies of the individual chips in the FH waveforms, the general signal model for embedding information in FH-MIMO radar was given in [27]. The general form of the vector of FH waveforms that exposes the information embedding parameters is

$$\Phi(t;n) = \sum_{q=0}^{Q-1} \mathrm{diag}\left(\mathbf{z}_q^{(n)} \odot e^{j\boldsymbol{\Omega}_q^{(n)}}\right)\exp\left\{j2\pi\mathbf{P}_q^{(n)}\mathbf{S}_q^{(n)}\mathbf{d}\Delta_f t\right\}\Pi_q(t), \tag{6}$$

where $\mathbf{z}_q^{(n)}$ denotes the vector of amplitudes of the M waveforms for the nth pulse, $\boldsymbol{\Omega}_q^{(n)}$ comprises constant phase rotations applied to the waveforms, $\odot$ denotes element-wise multiplication, and diag(·) returns a diagonal matrix. The matrix $\mathbf{S}_q^{(n)}$ gives a selection of M hops from the vector $\mathbf{d} \triangleq [0, 1, \cdots, K-1]^T$, while the matrix $\mathbf{P}_q^{(n)}$ expresses a permutation of the selected vector of M hops. Note that the vector of hop indices in the qth chip is $\mathbf{c}_q^{(n)} = \mathbf{P}_q^{(n)}\mathbf{S}_q^{(n)}\mathbf{d}$. Then we can see that varying $\mathbf{Z}_q^{(n)} \triangleq \text{diag}\left(\mathbf{z}_q^{(n)} \odot e^{j\mathbf{\Omega}_q^{(n)}}\right)$ provides for amplitude and phase modulation to be used. On the other hand, the selection matrix $\mathbf{S}_q^{(n)}$ can be used to implement the FHCS scheme [9], and the permutation matrix $\mathbf{P}_q^{(n)}$ allows for the index modulation via permutations [27] to be employed.

For the FHCS scheme considered in this work, information embedding is achieved by index modulation via carrier selection. In terms of (6), this means that only $\mathbf{S}_q^{(n)}$ is needed for its implementation. Thus, we can set $\mathbf{Z}_q^{(n)} = \mathbf{P}_q^{(n)} = \mathbf{I}_M$. The baseband representation of the transmitted signal during the nth pulse at spatial direction θ becomes

$$\mathbf{s}(t;n) = \mathbf{a}^T(\theta)\sum_{q=0}^{Q-1}\mathbf{S}_q^{(n)}\mathbf{h}(t)\Pi_q(t), \tag{7}$$

where

$$\mathbf{h}(t) = \exp\left\{j2\pi\mathbf{d}\Delta_f t\right\} = \left[1 \;\; e^{j2\pi\Delta_f t} \;\; \dots \;\; e^{j2\pi(K-1)\Delta_f t}\right]^T. \tag{8}$$

The FH codes $\mathbf{c}_q^{(n)}$ are drawn from a set of K hops, giving a total of $L = \binom{K}{M}$ combinations. Since L is in general not a power of two, the dictionary is truncated to $\tilde{L}$, which is the largest power-of-two integer not greater than L. We denote the truncated dictionary by $\tilde{\mathbb{L}}$. We assume that the communication receiver has the full knowledge of the dictionary $\tilde{\mathbb{L}}$.

The impact of the symbol embedding can be understood through the waveform AF [35] which characterizes the radar performance. The overall MIMO radar AF is defined as [33]

$$\chi(\tau, \nu) = \left|\sum_{m,m'=1}^{M}\chi_{m,m'}(\tau, \nu)\right|, \tag{9}$$

where the cross-ambiguity function (CAF) between waveforms $\phi_m(t)$ and $\phi_{m'}(t)$ is given by

$$\chi_{m,m'}(\tau, \nu) \triangleq \int_0^{T_\text{W}} \phi_m(t)\phi_{m'}^*(t+\tau)e^{j2\pi\nu t}dt. \tag{10}$$

When $m' = m$, expression (10) yields the auto-AF (AAF).

IV. Waveform Degeneration and Dictionary Balancing

Both the radar and communication performances of the FHCS scheme were discussed in [27]. In particular, embedding information in fast-time alters the radar AF as the hops making up the waveforms are varied. This issue was studied in [32] and the effect of waveform degeneration was explained. Specifically, waveform m in pulse n completely degenerates if symbol encoding at the radar selects Q symbols with a common hop in position m. Let the set $\mathbb{S}_k^{(m)} = \{\mathbf{s} \mid \mathbf{s}(m) = k\}$, where $0 \le k \le K-1$. Degeneration of waveform m happens if the communication function leads to the pulse being constructed from any of the sets $\mathbb{S}_k^{(m)}$. Note that, in addition to complete waveform degeneration, partial waveform degeneration results when the waveforms comprise subsets of repeated hops.

The likelihood of waveform degeneration can be reduced by balancing the occurrences and spread of the hops in $\tilde{\mathbb{L}}$ [32]. The first task is achieved during dictionary truncation by appropriately selecting the subset of $\tilde{L}$ symbols from $\mathbb{L}$. As the number of hops needed to make up the $\tilde{L}$ symbols in $\tilde{\mathbb{L}}$ is $M\tilde{L}$, by assuming $K = 2M$, which gives the largest number of combinations [9], the balancing procedure constructs the truncated dictionary such that each hop appears precisely $\tilde{L}/2$ times in $\tilde{\mathbb{L}}$. For the second task, we note that the communication symbols are encoded through the combination of hops. Therefore, balancing the spread of each hop over the waveforms is done by permuting the symbols in $\tilde{\mathbb{L}}$ which does not affect the communication function.

The balancing procedure described above is implemented at the design stage which yields an average performance improvement. However, for any particular waveform realization, the actual performance may not be optimal. Therefore, we propose a different approach where hop permutations within the symbols are used to optimize the performance for the specific communications data within the pulse. Furthermore, balancing the entire dictionary may not be a simple task if the dictionary is very large in size as would be the case for large K and M. For example of $K = 2M = 20$, we have a full dictionary of size L =184,756 symbols and the truncated dictionary is of size $\tilde{L} = 2^{17}$ = 131,072 symbols. For $Q = 5$, this gives a number of waveform realizations exceeding 3×10^{25}, making the enumeration of the set of waveforms and the balancing of the dictionary impractical.

As the proposed optimization procedure is now applied on a pulse basis, it is now both practical to implement and can yield improved performance. The problem is then to optimize the AAF and CAF with respect to the permutation matrices of the symbols comprising the pulses being readied for transmission. One strategy is to develop a suitable formulation that permits well-known convex optimization techniques to be recruited to find the optimal set of permutations. This, however, is a challenging task that is beyond the scope of this paper. Additionally, using convex optimization approaches would be computationally prohibitive for real-time implementation. Therefore, we proceed here to develop a heuristic strategy that leads to a suboptimal but useful solution. Since we are focused on a particular pulse, we drop the superscript $^{(n)}$ for notational simplicity in the sequel.

V. Proposed Pulse Balancing Strategy

The overall AF in (9) is the sum of all AAFs and CAFs. Substituting (4) into it, we find that the total AF includes all pairwise combinations of hops in the pulse. Therefore, expression (9) is insensitive to the permutations of the hops within the symbols and, therefore, cannot be used as a measure for balancing them. Consequently, we consider the individual AFs of (10) instead and focus on their zero-Doppler slices. Furthermore, in order to facilitate the development of the balancing strategies, we look at the AFs for delays that are integer multiples of the chip duration, that is, we evaluate the AFs for $\tau = l\Delta_t$, for $l = 0, \dots, Q-1$. The orthogonality of the hops over the chip duration then implies that the CAF for a pulse can be expressed as

$$\chi_{m,m'}(l) = \int_0^{T_W} \phi_m(t)\phi^*_{m'}(t + l\Delta_t)dt = \sum_{q=0}^{Q-l-1} \delta\left(\mathbf{c}_q(m), \mathbf{c}_{q+l}(m')\right). \tag{11}$$

Let the matrix delta function be the Dirac delta applied to the matrix element-wise. That is, $[\boldsymbol{\delta}(\mathbf{A})]_{i,j} = \delta([\mathbf{A}]_{i,j})$, where $[\mathbf{A}]_{i,j}$ is the (i, j)th element of $\mathbf{A}$. Then we can combine the various AAFs and CAFs into a single matrix $\chi(l)$, given by

$$\chi(l) = \sum_{q=0}^{Q-l-1} \boldsymbol{\delta}\left(\mathbf{c}_{q+l} - \mathbf{c}_q^T\right), \tag{12}$$

where the difference operation of the column and row vectors returns a matrix with difference of all pairs of elements of the two vectors. Assuming without loss of generality that appropriate normalization is used so that the energy per chip is 1, perfectly orthogonal waveforms give

$$\chi(l) = \begin{cases} Q\mathbf{I}, & \text{for } l = 0, \\ \mathbf{0}, & \text{otherwise.} \end{cases} \tag{13}$$

Now when FHCS encoding is used in the DFRC context, $\chi(0)$ remains diagonal but $\chi(l)$ would no longer be $\mathbf{0}$ for $l > 0$ due to repetitions of the hops. As the contributions resulting from the repetitions are dictated by the symbols used, only their ordering within the symbols may be manipulated. Thus, the goal of the balancing strategy is to permute the symbols in order to spread the non-zero contributions of repeated hops over the entries of $\chi(l)$ as evenly as possible.

For the task of finding the optimal hop arrangement within the Q symbols or, equivalently, determining the $Q - 1$ permutation matrices, considering all l delays from 1 to $Q - 1$ is difficult even for heuristic approaches. Noting however that the largest sidelobe is obtained for $l = 1$, we simplify the problem by restricting our attention to $\chi(1)$. The balancing strategy then aims to find a set of symbol permutations that gives the most even spread of the entries of $\chi(1)$. This problem may be solved using an exhaustive search only for small enough scenarios (that is small K and Q). More generally, we present a heuristic algorithm that returns a sub-optimal solution by working on the symbols in the pulse in sequence. The solution is suboptimal in the sense that it returns either

The steps of the balancing algorithm are summarized in Algorithm 1. Let $\{\mathbf{c}_1, \mathbf{c}_2, \ldots, \mathbf{c}_Q\}$ be the set of symbols chosen by the communications function to make up the current pulse. Since the permutation of the first symbol leads to a permutation of the entire pulse, we start from symbol 2. Thus, for each symbol $q \in \{2, \ldots, Q - 1\}$, we obtain the matrix $\mathbf{C}_s = \boldsymbol{\delta}\left(\mathbf{c}_q - \mathbf{c}^T_{q+l}\right)$ which gives the contributions of symbols q and $q + 1$ to the AFs. ALso let $\mathbf{C}_a$ be the total contributions matrix for symbols 1 to $q - 1$ and $\mathbf{C}_t = \mathbf{C}_a + \mathbf{C}_s$ be the overall contributions matrix up to symbol $q + 1$. Now, the matrix $\mathbf{C}_s$ has entries that are either 0 or 1 and contains at most one non-zero entry per row and column. Then, for each of

Algorithm 1: Pulse balancing via symbol permutations

Input : Pulse comprising Symbols $\{\mathbf{c}_1, \mathbf{c}_2, \ldots, \mathbf{c}_Q\}$

1 **for** $q = 2 : Q - 1$ **do**

2 Calculate $\mathbf{C}_a = \sum_{l=1}^{q} \boldsymbol{\delta}\left(\mathbf{c}_{l-1} - \mathbf{c}_l^T\right)$, and $\mathbf{C}_s = \boldsymbol{\delta}\left(\mathbf{c}_q - \mathbf{c}^T_{q+1}\right)$

3 Put $\mathbf{C}_t = \mathbf{C}_a + \mathbf{C}_s$

4 Let $\mathbf{r} = \mathbf{C}_t\mathbf{1}_M$ and $\mathbf{u} = \mathbf{1}_M^T\mathbf{C}_t$ be the vectors comprising the sum of the rows and columns of $\mathbf{C}_t$, and put

$$(\hat{r}, \hat{j}) = \max \mathbf{r}, \text{ and } (\check{r}, \check{j}) = \min \mathbf{r},$$
$$(\hat{u}, \hat{\imath}) = \max \mathbf{u}, \text{ and } (\check{u}, \check{\imath}) = \min \mathbf{u}$$

5 Compute $\hat{v} = \max \mathbf{C}_t$ and $\check{v} = \min \mathbf{C}_t$

6 **if** $(\hat{r} - \check{r} > 1)$ **then**

7 Swap $\hat{j}$-th and $\check{j}$-th rows of $\left\{\mathbf{c}_1, \ldots, \mathbf{c}_{q-1}\right\}$

8 **else if** $(\hat{u} - \check{u} > 1)$ **then**

9 Swap $\hat{\imath}$-th and $\check{\imath}$-th rows of $\left\{\mathbf{c}_{q+1}, \ldots, \mathbf{c}_Q\right\}$

10 **else if** $(\hat{v} - \check{v} > 1)$ **then**

11 find a suitable place to swap entry $\hat{v}$ to by suitably swapping rows of $\left\{\mathbf{c}_1, \ldots, \mathbf{c}_{q-1}\right\}$ and columns of $\left\{\mathbf{c}_{q+1}, \ldots, \mathbf{c}_Q\right\}$

12 **end**

Output : Balanced symbols $\{\mathbf{c}_1, \mathbf{c}_2, \ldots, \mathbf{c}_Q\}$

the non-zero entries of $\mathbf{C}_s$, the algorithm checks whether the corresponding entry in $\mathbf{C}_t$ exceeds another entry by more than 1. This indicates that a better spread of the contributions is obtained. Consequently, the algorithm looks for another slot to move this non-zero entry to. This is achieved by either swapping rows or columns or both. A row swap can be achieved by swapping the corresponding entries of symbols 1 to $q - 1$, whereas a column swap can be obtained by swapping the corresponding entries in symbols $q + 1$ to Q. Note that the algorithm also looks to ensure adequate distribution of the non-zero entries over the rows and columns in steps 6 and 8 of the algorithm.

VI. Numerical Results

The performance of the proposed balancing procedure is compared to the unbalanced dictionary as well as to the strategy presented in [32]. To this end, we consider a MIMO radar platform comprising $M = N = 3$ colocated transmit and receive antennas where each waveform comprises $Q = 5$ subpulses. The radar operates at a center frequency of 8 GHz and a bandwidth of $BW = 20$ MHz. The duty cycle is set to 2% and the PRF to 20 kHz. $K = 6$ different frequency hops are used giving a total of $L = 20$ different symbols. Thus, the dictionary truncation to the highest power-of-two integer not greater than L gives a codebook of length $\tilde{L} = 16$.

The auto and cross ambiguity functions, AAF and CAF respectively, are shown for the direct truncation dictionary, the balanced dictionary and the pulse balancing strategy. For the latter, the balancing through exhaustive search is shown along with the output of the heuristic approach. The curves are labeled as ‘DIR’ for the direct truncation, ‘DBAL’ for the dictionary balancing, ’PBAL-OPT’ for the solution resulting from the exhaustive search and ’PBAL’ for the output of the heuristic algorithm. Looking at the AAFs in Figs. 1-3, we see

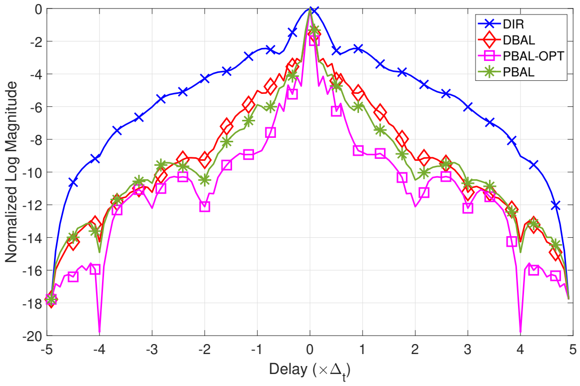

Fig. 1: Zero-Doppler slice of the AAF for waveform 1 ($K = 6$).

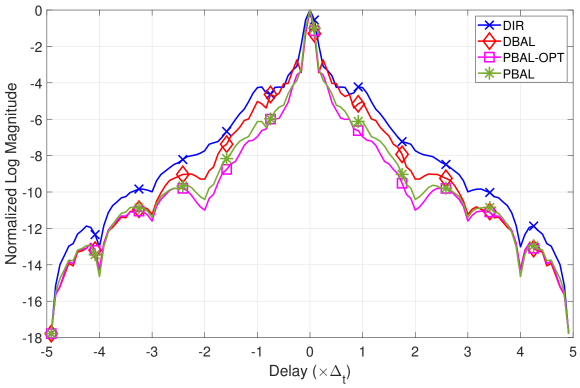

Fig. 2: Zero-Doppler slice of the AAF for waveform 2 ($K = 6$).

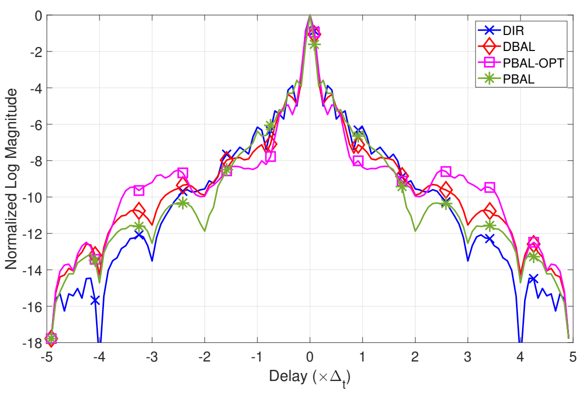

Fig. 3: Zero-Doppler slice of the AAF for waveform 3 ($K = 6$).

that the proposed strategy improves on the dictionary balancing, which itself performs better than the direct truncation. The amount of improvement varies between the waveforms and is greatest for waveform 1. This is due to the fact that waveform 1 obtained from the direct truncation dictionary is poor due to the high repetition rate of hop 1 (see [32]). Turning to the CAFs, which are shown in Figs. 4-6, we observe that the balancing strategies have higher sidelobes of the CAFs, which is the cost incurred for lowering the sidelobes of the

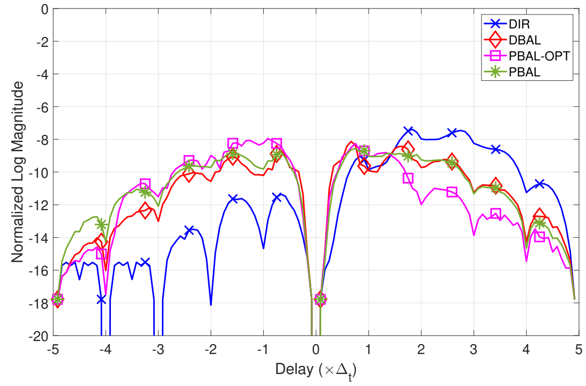

Fig. 4: Zero-Doppler slice of the CAF for waveforms 1 and 2 ($K = 6$).

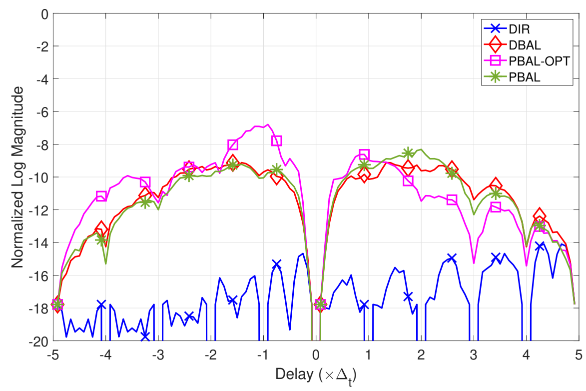

Fig. 5: Zero-Doppler slice of the CAF for waveforms 1 and 3 ($K = 6$).

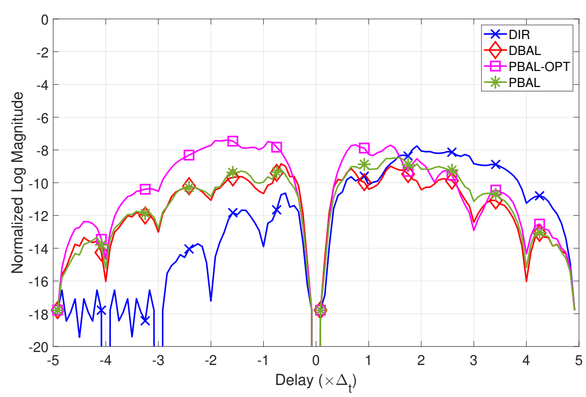

Fig. 6: Zero-Doppler slice of the CAF for waveforms 2 and 3 ($K = 6$).

AAFs. However, the CAFs are still mostly below -8dB while the AAFs are reduced significantly, particularly for waveform 1.

Finally, two remarks are in order: First, the improvement is expected to become more significant for larger scenarios, that is for increasing K and Q. Second, the gap between the optimum and heuristic approaches indicates that further gains can be achieved by improving the algorithm. Furthermore, solving the full optimization problem, which is beyond the scope of this work, would lead to improved overall AF profiles by taking all delays into account.

VII. Conclusion

The symbol dictionary selection in the FH-DFRC scheme has a direct impact on the performance of the radar. In this paper, we studied this problem in terms of the effect of the information embedding on the AAFs and CAFs of the resulting waveforms. We showed that balancing the pulse leads to improved performance over the dictionary balancing. This improvement was demonstrated fora a small scenario using the exhaustive search. Furthermore, we presented a heuristic approach was presented that allows suboptimal pulse balancing to be achieved for larger scenarios.

References

[1] A. Hassanien, M. G. Amin, E. Aboutanios, and B. Himed, "Dual-function radar communication systems: A solution to the spectrum congestion problem," *IEEE Signal Processing Magazine*, vol. 36, no. 5, pp. 115–126, 2019.

[2] B. Paul, A. R. Chiriyath, and D. W. Bliss, "Survey of RF communications and sensing convergence research," *IEEE Access*, vol. 5, pp. 252–270, 2016.

[3] S. Mazahir, S. Ahmed, and M.-S. Alouini, "A survey on joint communication-radar systems," *Frontiers in Communications and Networks*, vol. 1, p. 619483, 2021.

[4] A. Hassanien, M. G. Amin, Y. D. Zhang, and F. Ahmad, "Dual-function radar-communications: Information embedding using sidelobe control and waveform diversity," *IEEE Transactions on Signal Processing*, vol. 64, no. 8, pp. 2168–2181, April 2016.

[5] E. BouDaher, A. Hassanien, E. Aboutanios, and M. G. Amin, "Towards a dual-function mimo radar-communication system," in *2016 IEEE Radar Conference (RadarConf)*, May 2016, pp. 1–6.

[6] C. Sahin, J. Jakabosky, P. M. McCormick, J. G. Metcalf, and S. D. Blunt, "A novel approach for embedding communication symbols into physical radar waveforms," in *2017 IEEE Radar Conference (RadarConf)*, May 2017, pp. 1498–1503.

[7] A. Hassanien, B. Himed, and B. D. Rigling, "A dual-function MIMO radar-communications system using frequency-hopping waveforms," in *2017 IEEE Radar Conference (RadarConf)*, May 2017, pp. 1721–1725.

[8] A. Hassanien, E. Aboutanios, M. G. Amin, and G. A. Fabrizio, "A dual-function MIMO radar-communication system via waveform permutation," *Digital Signal Processing*, vol. 83, pp. 118 – 128, 2018.

[9] W. Baxter, E. Aboutanios, and A. Hassanien, "Dual-function MIMO radar-communications via frequency-hopping code selection," in *2018 52nd Asilomar Conference on Signals, Systems, and Computers*, 2018, pp. 1126–1130.

[10] H. Nosrati, E. Aboutanios, and D. Smith, "Array partitioning for multi-task operation in dual function MIMO systems," *Digital Signal Processing*, vol. 82, pp. 106–117, Nov. 2018.

[11] A. Ahmed, Y. D. Zhang, A. Hassanien, and B. Himed, "OFDM-based joint radar-communication system: Optimal sub-carrier allocation and power distribution by exploiting mutual information," in *2019 53rd Asilomar Conference on Signals, Systems, and Computers*, Nov. 2019, pp. 559–563.

[12] J. Euzière, R. Guinvarc'h, M. Lesturgie, B. Uguen, and R. Gillard, "Dual function radar communication time-modulated array," in *2014 International Radar Conference*, Oct. 2014, pp. 1–4.

[13] A. Hassanien, M. G. Amin, Y. D. Zhang, and B. Himed, "A dual-function MIMO radar-communications system using PSK modulation," in *2016 24th European Signal Processing Conference (EUSIPCO)*, Aug. 2016, pp. 1613–1617.

[14] I. P. Eedara, A. Hassanien, M. G. Amin, and B. D. Rigling, "Ambiguity function analysis for dual-function radar communications using PSK signaling," in *2018 52nd Asilomar Conference on Signals, Systems, and Computers*, Oct. 2018, pp. 900–904.

[15] F. Liu, C. Masouros, A. P. Petropulu, H. Griffiths, and L. Hanzo, "Joint radar and communication design: Applications, state-of-the-art, and the road ahead," *IEEE Transactions on Communications*, vol. 68, no. 6, pp. 3834–3862, 2020.

[16] A. Hassanien, M. G. Amin, Y. D. Zhang, and B. Himed, "A dual-function MIMO radar-communications system using PSK modulation," in *2016 24th European Signal Processing Conference (EUSIPCO)*, 2016, pp. 1613–1617.

[17] A. Hassanien, M. G. Amin, Y. D. Zhang, F. Ahmad, and B. Himed, "Non-coherent PSK-based dual-function radar-communication systems," in *2016 IEEE Radar Conference (RadarConf)*, May 2016, pp. 1–6.

[18] A. Hassanien, M. G. Amin, Y. D. Zhang, and F. Ahmad, "A dual function radar-communications system using sidelobe control and waveform diversity," in *2015 IEEE Radar Conference (RadarCon)*, May 2015, pp. 1260–1263.

[19] ——, "Efficient sidelobe ASK based dual-function radar-communications," in *SPIE Radar Sensor Technology XX*, vol. 9829, no. 98290K, April 2016, pp. 1–11.

[20] X. Wang, A. Hassanien, and M. G. Amin, "Dual-function MIMO radar communications system design via sparse array optimization," *IEEE Transactions on Aerospace and Electronic Systems*, vol. 55, no. 3, pp. 1213–1226, 2018.

[21] H. Nosrati, E. Aboutanios, and D. Smith, "Array partitioning for multi-task operation in dual function MIMO systems," *Digital Signal Processing*, vol. 82, pp. 106–117, 2018.

[22] Y. Yao, X. Li, and L. Wu, "Cognitive frequency-hopping waveform design for dual-function MIMO radar-communications system," *Sensors*, vol. 20, no. 20, pp. 1–21, 2020.

[23] X. Wang, J. Xu, A. Hassanien, and E. Aboutanios, "Joint communications with FH-MIMO radar systems: An extended signaling strategy," in *2021 IEEE International Conference on Acoustics, Speech and Signal Processing (ICASSP)*, 2021, pp. 8253–8257.

[24] J. Xu, X. Wang, E. Aboutanios, and G. Cui, "Hybrid index modulation for dual-functional radar communications systems," *IEEE Transactions on Vehicular Technology*, pp. 1–15, 2022.

[25] I. P. Eedara and M. G. Amin, "Dual function FH MIMO radar system with DPSK signal embedding," in *2019 27th European Signal Processing Conference (EUSIPCO)*, 2019, pp. 1–5.

[26] K. Wu, J. A. Zhang, X. Huang, and Y. J. Guo, "Integrating secure communications into frequency hopping MIMO radar with improved data rate," *IEEE Transactions on Wireless Communications*, vol. 21, no. 7, pp. 5392–5405, 2022.

[27] W. Baxter, E. Aboutanios, and A. Hassanien, "Joint radar and communications for frequency-hopped MIMO systems," *IEEE Transactions on Signal Processing*, vol. 70, pp. 729–742, 2022.

[28] A. Hassanien, M. G. Amin, E. Aboutanios, and B. Himed, "Dual-function radar communication systems: A solution to the spectrum congestion problem," *IEEE Signal Processing Magazine*, vol. 36, no. 5, pp. 115–126, Sep. 2019.

[29] I. P. Eedara, A. Hassanien, M. G. Amin, and B. D. Rigling, "Ambiguity function analysis for dual-function radar communications using PSK signaling," in *2018 52nd Asilomar Conference on Signals, Systems, and Computers*, Oct. 2018, pp. 900–904.

[30] I. Eedara, A. Hassanien, and M. Amin, "Performance analysis of dual-function multiple-input multiple-output radar-communications using frequency hopping waveforms and phase shift keying signalling," *IET Radar, Sonar, & Navigation*, vol. 15, pp. 402–418, 2021.

[31] I. P. Eedara, M. G. Amin, A. Hoorfar, and B. K. Chalise, "Dual-function frequency-hopping MIMO radar system with CSK signaling," *IEEE Transactions on Aerospace and Electronic Systems*, vol. 58, no. 3, pp. 1501–1513, 2022.

[32] W. Baxter, H. Nosrati, and E. Aboutanios, "A study on the performance of symbol dictionary selection for the frequency hopped DFRC scheme," in *2020 IEEE Radar Conference (RadarConf)*, 2020, pp. 1–6.

[33] C.-Y. Chen and P. Vaidyanathan, "MIMO radar ambiguity properties and optimization using frequency-hopping waveforms," *IEEE Transactions on Signal Processing*, vol. 56, no. 12, pp. 5926–5936, 2008.

[34] M. I. Skolnik, *RADAR Systems*. McGraw-Hill, 2001.

[35] G. San Antonio, D. R. Fuhrmann, and F. C. Robey, "MIMO radar ambiguity functions," *IEEE Journal of Selected Topics in Signal Processing*, vol. 1, no. 1, pp. 167–177, 2007.